Dev Genes Evol (1998) 208:117–127

ORIGINAL ARTICLE

Nai-Jia L. Liu · Deborah E. Isaksen
Constance M. Smith · David A. Weisblat

Movements and stepwise fusion of endodermal precursor cells in leech

Received: 14 October 1997 / Accepted: 4 February 1998

Abstract At the four-cell stage, embryos of glossiphoniid leeches comprise identified blastomeres A, B, C and D. Subsequent cleavages of the A, B and C quadrants yield three large, yolk-rich endodermal precursor cells, macromeres A‴, B‴ and C‴. Eventually, these cells generate the epithelial lining of the gut via cellularization of a multinucleate syncytium. Meanwhile, cleavage in the D quadrant generates ten teloblasts that give rise to segmental mesoderm and ectoderm via stem cell divisions. Here we show that, during cleavage, macromeres A‴, B‴ and C‴ shift clockwise relative to the D quadrant, while C‴ comes to envelop the nascent teloblasts. During gastrulation, derivatives of the teloblasts undergo epibolic movements over the surface of the A‴, B‴ and C‴ macromeres to form the germinal plate, from which segmental tissues arise. We find that the three macromeres fuse in a stepwise manner to initiate formation of the multinucleate syncytium; cell C‴ fuses about 25 h after the fusion of A‴ and B‴, and the teloblasts fuse with the macromere-derived syncytium later still. When macromeres are biochemically arrested by microinjecting them with the A chain of ricin, a further difference among the macromeres is revealed. Biochemical arrest of A‴ or B‴ slightly retards the rate of germinal plate formation, but arrest of C‴ frequently accelerates this process.

Key words Annelida · Leech · Cell fusion · Endoderm · Macromeres

Edited by D. Tautz

N.-J. L. Liu[1] · D.E. Isaksen · C.M. Smith[2] · D.A. Weisblat (✉)
Department of Molecular and Cell Biology, 385 LSA,
University of California, Berkeley, CA 94720-3200, USA

Current addresses:
[1] Department of Biology, University of California at San Diego,
La Jolla, CA 92039, USA
[2] Department of Cell Biology,
Emory University School of Medicine, Atlanta,
GA 30322-3030, USA

Introduction

During gastrulation, cells undergo extensive positional rearrangements to establish the adult body plan. In embryos of glossiphoniid leeches such as *Helobdella robusta*, gastrulation entails the epibolic movements of mesodermal and ectodermal progenitor cells over three large, yolky endodermal precursor cells, macromeres A‴, B‴ and C‴ (Nardelli-Haefliger and Shankland 1993; Smith et al. 1996). We report here that the macromeres undergo stepwise cell fusions and marked positional changes prior to and during epiboly.

Prior to epiboly in *Helobdella*, stereotyped cleavages produce three types of cells, macromeres, micromeres and teloblasts. Blastomeres A, B and C of the four-cell embryo each generate 1 large *macromere* and 3 small *micromeres* (9 in total) while blastomere D generates 5 pairs of intermediate-sized *teloblasts*, and 16 additional micromeres (Fig. 1, stages 2–7; Whitman 1878; Sandig and Dohle 1988; Bissen and Weisblat 1989). Telobasts are stem cells that generate precursors of segmental mesodermal and ectoderm. During gastrulation, teloblasts generate bilaterally paired arrays (*germinal bands*) of segmental founder cells (*blast cells*) in prospective dorsal territory, near the animal pole of the embryo (Fig. 1, stage 8 early). The germinal bands move ventrovegetally over the surface of the macromeres and coalesce from anterior to posterior along the ventral midline, forming the *germinal plate* (Fig. 1, stage 8–9), from which segmental mesoderm and ectoderm arise. Concurrent with the movements of the germinal bands, a squamous epithelium, which covers the germinal bands and the area between them, spreads over the embryo. This epithelium is derived from the micromeres, which arise near the animal pole in the prospective anterodorsal regions of the embryo (Fig. 1, stages 4–7; Weisblat et al. 1984; Smith and Weisblat 1994).

In accord with the germ layer theory, C.O. Whitman (1878) proposed that the three macromeres (A‴, B‴ and C‴) are endodermal progenitors. This was confirmed by Nardelli-Haefliger and Shankland (1993), who found, as

did Bychowsky (1921), that the macromeres generate a single multinucleate syncytium, which then cellularizes to form the epithelial lining of the gut. Forming a single syncytium from three macromeres requires that these cells fuse.

Here, we have characterized the behavior of the macromeres during stages 4–9. We find that the macromeres undergo marked positional changes and fuse in a stereotypic, stepwise manner. A‴ and B‴ fuse first, to form a syncytial A/B cell; 25 h later, C‴ fuses with A/B to form cell A/B/C. To test for their role in germinal plate formation, individual macromeres were injected with the A chain of ricin, a protein synthesis inhibitor. While embryos in which A‴ or B‴ was injected with ricin exhibited a slight retardation of germinal band coalescence, embryos in which C‴ was injected with ricin frequently exhibited markedly accelerated coalescence.

Materials and methods

Embryos

H. robusta embryos were obtained and maintained as described previously (Smith and Weisblat 1994). The embryonic staging system and cell lineage nomenclature are as described by Stent et al. (1992). Accordingly, macromeres, teloblast precursors and teloblasts are represented by uppercase letters, while blast cells and micromeres are designated by lowercase letters corresponding to the parent blastomere. Primes (′) further designate the birth order of micromeres; thus, the three micromere-producing divisions of the A blastomere yield micromeres a′, a″ and a‴, and macromeres A′, A″ and A‴, respectively. Embryonic ages during stages 7–8 are given more precisely as hours since stage 6a (Smith and Weisblat 1994).

Microinjections

To analyze the shapes, positions and fusion processes of macromeres, cells of interest were micro-injected (Smith and Weisblat 1994) with a solution consisting of approximately 15 mg/ml β-galactosidase, 1% fast green, 50 mM KCl and 20 mM TRIS-HCl, pH 7.5. To fill micropipes (FHC #30-30-0) with this viscous solution, they were first back-filled with 0.5 µl of distilled water, then with approximately 0.8 µl of a 3/2 mixture of β-galactosidase (40 mg/ml in 50 mM TRIS-HCl, pH 7.5) and fast green (4% in 200 mM KCl) and stored overnight at 4° C to allow the enzyme-dye mixture to equilibrate.

To perturb gastrulation, cells in stage 6a embryos were injected with an aqueous solution of ricin A chain (0.45 mg/ml; Sigma) in 50 mM KCl, 1% fast green. To facilitate measuring germinal plate formation in such embryos, the left mesodermal teloblast was injected, at about stage 6a, with rhodamine dextran amine (RDA) as described (Nardelli-Haefliger and Shankland 1993), so that all but the first four m blast cell clones would be labeled. Embryos were fixed at stage 6a+75 h, by which time control embryos had reached mid stage 8.

In experiments designed to look for ultrastructural correlates of A‴–B‴ fusion, fusion was monitored by injecting fluorescein dextran amine (FDA) as described (Nardelli-Haefliger and Shankland 1993) into A‴ prior to stage 6. Live embryos were scored for A‴–B‴ fusion at stage 6a+41 h using epifluorescence to assess the distribution of the injected tracer, then processed for electron microscopy (see below).

Histochemistry

To visualize micro-injected β-galactosidase, embryos were fixed for 30 min (1% glutaraldehyde in 100 mM sodium citrate), then rinsed for 30 min [5 mM $K_3Fe(CN)$, 5 mM $K_4Fe(CN)_6$, 1 mM $MgCl_2$, 0.2% Triton in 100 mM sodium citrate]. For staining, the embryos were transferred to a fresh aliquot of the rinse solution to which X-gal (5-bromo-4-chloro-3-indolyl-β-D-galactopyranoside; Sigma; 2% in DMF) had been added to a final concentration of 0.1%. The color reaction was allowed to proceed overnight in the dark at ambient temperature. Stained embryos were rinsed 3 times with 100 mM sodium citrate, then dehydrated through a graded ethanol series and cleared in a 3/2 mixture of benzyl benzoate/benzyl alcohol.

Embryos in which cells had been injected with RDA were fixed at selected time points in a solution of 4% formaldehyde in 100 mM TRIS-HCl, pH 7.5–8.0 for 1 h at ambient temperature, rinsed in 100 mM TRIS-HCl, dehydrated and cleared as described above.

Light microscopy and photography

Embryos labeled with β-galactosidase or RDA were viewed under DIC optics or by fluorescence microscopy (Zeiss Axiophot) and photographed using Ektachrome 160 or 400 film (Kodak), respectively. For the embryos shown in Fig. 7, images at different focal planes were obtained with an integrating color CCD camera (Dage DC-330), digitized (Scion LG-3) and processed to generate photomontages (NIH Image 1.6; Adobe Photoshop 4.0).

Electron microscopy

Embryos were fixed for 2 h at 4° C in 2% glutaraldehyde, 0.5% osmium tetroxide in 60 mM sodium cacodylate (pH 7.2) made by mixing buffered 4% glutaraldehyde and 1% osmium tetroxide just before use (Hirsch and Fedorko 1968). Embryos were rinsed several times' first with 100 mM sodium cacodylate (pH 7.2), then with distilled, deionized water, and post-stained (0.5% uranyl acetate) for 1 h at 4° C in the dark. Embryos were dehydrated in an acetone series, embedded in Epon-Spurr resin (Demaree et al. 1995) and cured at 70° C for 2 days.

Alternating series of thick (~800 nm) and thin (50 nm) serial sections were cut (UC Berkeley Electron Microscope Laboratory). Thick sections were stained with toluidine blue and viewed by light microscopy to identify relevant portions of the embryo for examination by electron microscopy. Selected thin sections were then placed on Formvar-coated slot grids, counter-stained with uranyl acetate and lead citrate, and examined on a JEOL 100CX transmission electron microscope.

Results

Movements and cell fusion among macromeres during normal gastrulation

The work presented here describes four phases of macromere movements and cell fusions that take place during stages 3–9. Describing cell movements during this period is complicated by the fact that the mutually orthogonal animal-vegetal and B-D axes of the cleavage stages (Fig. 1, stages 4a and 7) do not map simply to the anteroposterior and dorsoventral axes that arise during gastrulation (Fig. 1, early stage 8 and stage 9). The prospective anterior end of the leech corresponds to the animal pole of the early embryo. The prospective posterior end, how-

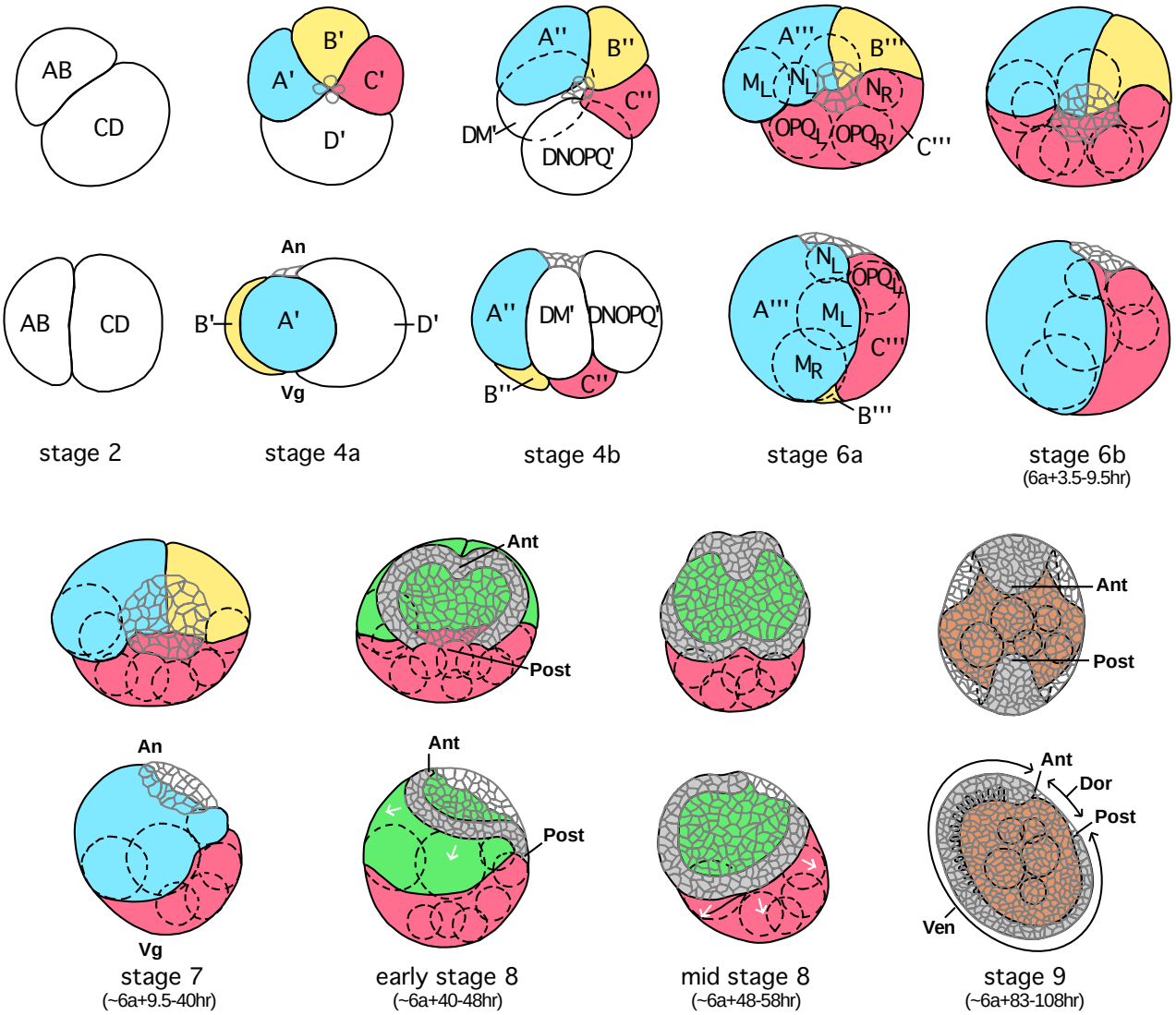

Fig. 1 Summary of leech development. Selected stages (Stent et al. 1992) are depicted as seen from the animal pole (*top rows* prospective dorsal views; posterior *toward the bottom*) and from the left side (*bottom rows* prospective sagittal views; posterior *to the right*). The A, B and C quadrant macromeres are shaded *blue*, *yellow* and *orange*, respectively. Later stages are also designated in terms of hours of development after the beginning of stage 6a. Animal views of stages 4b-7 show the clockwise expansion of A‴/A‴, B‴/B‴ and C‴/C‴ relative to the D quadrant. B′ straddles the midline in stage 4a, but by stage 6-7, B‴ lies contralateral to A‴. C‴ shifts clockwise as it comes to envelop most of the proteloblasts and teloblasts (DM′, DNOPQ′, OPQ, M and N are labeled in some stages) arising from D′. A‴ and B‴ fuse during early stage 8 to form cell A/B (*green*). Left equatorial views of stages 6a-8 illustrate the shift of the macromeres relative to the animal-vegetal (*An-Vg*) axis: A‴, B‴ and later A/B occupy animal territory while C‴ occupies vegetal territory. By the end of stage 7, the germinal bands (*grey*) are joined at their anterior (*Ant*) ends and elongate through the addition of blast cells from the teloblasts at their posterior (*Post*) ends. During stage 8, they move ventrovegetally over the surface of the embryo (*arrows*) and gradually coalesce from anterior to posterior, forming the germinal plate (*grey*) along the ventral (*Ven*) midline. B stage 9, germinal plate formation is complete and C‴ has fused with A/B to form the syncytial volk cell A/B/C (*brown*); dorsal (*Dor*) territory is indicated

ever, is defined by the proximal ends of the germinal bands, rather than by the vegetal pole. Because the germinal plate wraps around much of the stage 8 embryo, both the vegetal pole and the territory occupied by the B cell in the stage 4a embryo correspond to prospective ventral territory. Thus, viewing the stage 4a embryo from the animal pole with the B quadrant at the top corresponds roughly to a dorsal view of an older embryo with anterior at the top (Fig. 1, stage 4a versus stages 8–9).

Phase I: clockwise expansion of macromeres (stage 3 to stage 7)

To follow the changes in shape and position of the macromeres during these stages, we examined embryos in which individual macromeres had been injected with β-galactosidase (Fig. 2). In four-cell embryos (stage 3), each blastomere extends from the animal pole to the vegetal pole. Thus, the shape of the cells approximates quadrants of a sphere that intersect along the animal-vegetal axis of the embryo. The A, B and C quadrant mac-

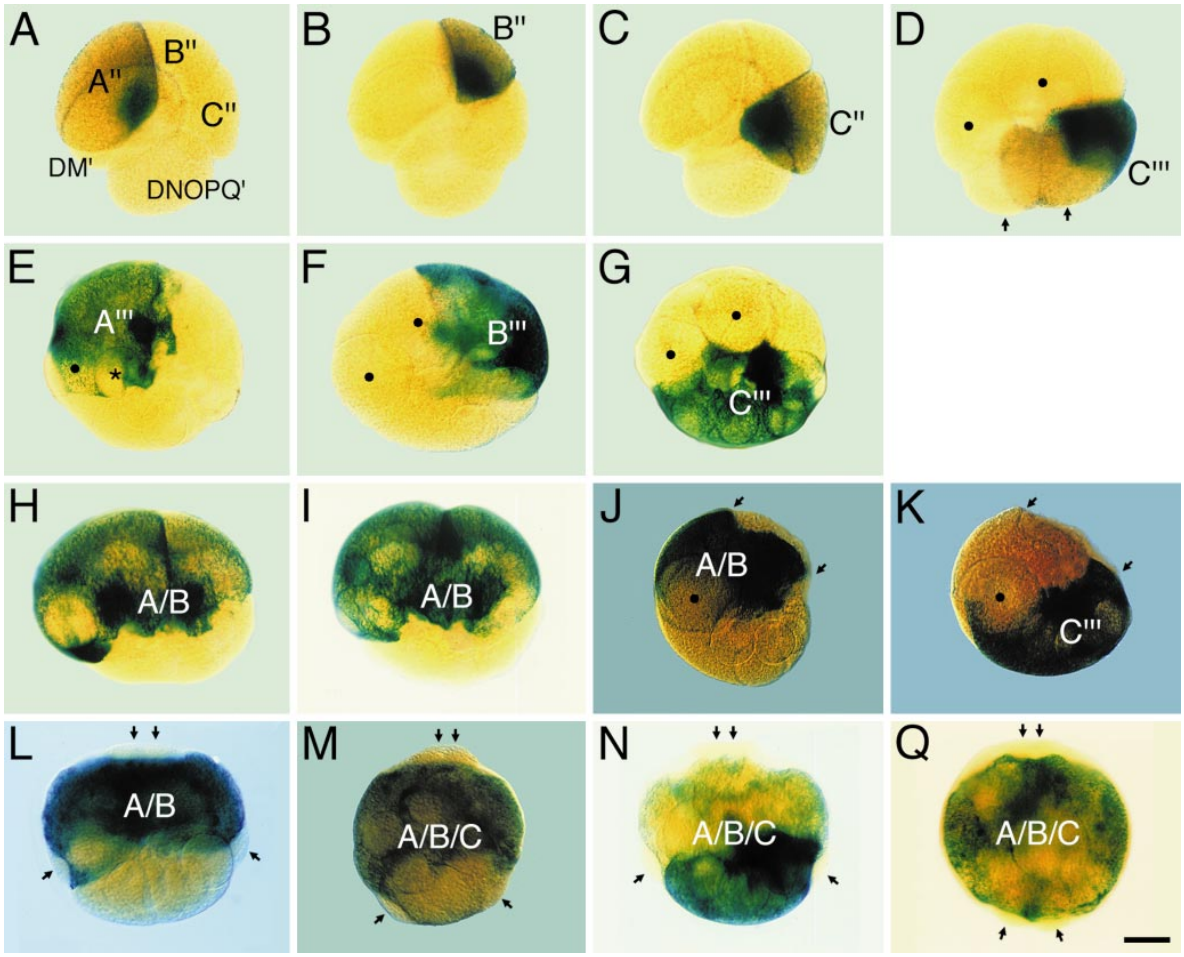

Fig. 2A–Q Shape and positional changes and cell fusion of the macromeres. Photomicrographs of embryos, fixed and stained at various stages, in which macromeres of quadrant A, B or C had been injected with β-galactosidase at either stage 4b or 5. Unless noted, all views are of the animal pole. **A**–**C** A″, B″ and C″, respectively, have relatively simple shapes at stage 4b. **D** A stage 5 embryo in which C‴ had been injected; DM and DNOPQ have given rise to the M teloblasts (*dots*) and NOPQ proteloblasts (*arrows*). C‴ covers half of the surface of $NOPQ_R$ at the animal side (*dark blue*) but has spread much further at the vegetal side (*light blue*), covering all of $NOPQ_R$ and half of $NOPQ_L$. **E**–**G** A‴, B‴ and C‴, respectively, in mid stage 7 embryos (stage 6a+21–25 h) are irregularly shaped and have undergone a clockwise expansion, but still have not fused, as evidenced by the fact that the injected β-galactosidase did not cross from one cell to another. Together, A‴, B‴ and C‴ cover most of the embryo surface. The thickness of the macromeres over the underlying teloblasts is evidenced by the intensity of the blue reaction product; N_L (*asterisk*) and both M teloblasts (*dots*) are labeled. **H** Early A‴–B‴ fusion in a stage 7 embryo (stage 6a+38 h); β-galactosidase injected into A‴ had leaked into B‴ but had not yet equilibrated, as evidenced by the difference in the intensity of staining. **I** Later A‴–B‴ fusion in a similar embryo; β-galactosidase staining is uniform throughout A/B. C‴ and teloblasts remained completely unstained, and germinal bands are visible as clear regions overlying A/B. **J**, **K** Left lateral views of early stage 8 embryos (stage 6a+42 h) after A‴–B‴ fusion. A/B occupies most of the region under the micromere cap (*bounded by arrows*), having retracted from the vegetal pole to about the level of the M_L teloblast (*dot*). C‴ had receded from the micromere cap and occupies vegetal territory. **L**–**Q** A/B–C‴ fusion in stage 8 embryos. Germinal bands (*single arrows*) and anterior germinal plate (*double arrows*) are visible at the edge in each embryo. **L** Ventral view prior to A/B–C‴ fusion. **M**, **N** Early A/B–C‴ fusion; dorsal views of embryos at stage 6a+72 h at the start of A/B–C‴ fusion. β-galactosidase had started to diffuse from A/B into C‴ (**M**) and from C‴ into A/B (**N**). **Q** Late A/B–C‴ fusion; ventral view of an embryo at stage 6a+75 h in which C‴ had been injected. The reaction product is distributed uniformly throughout A/B/C, but underlying, unfused teloblasts give a blotchy appearance to the embryo (*Scale bar* 100 μm)

romeres keep their approximate shape through stage 4 (Fig. 2A–C). During this time, each macromere generates three micromeres, after which they are designated as A‴, B‴ and C‴. The nine micromeres from quadrants A–C contribute little to the overall geometry of the embryo due to their small, flattened shapes.

The simple geometry of the four-cell stage is gradually disrupted by cleavages of the D quadrant derivatives. During stages 4–6, blastomere D is transformed into 10 spherical teloblasts (Fig. 1); 16 micromeres also arise from the D quadrant during this period, but like the A–C quadrant micromeres, they contribute little to the overall shape of the embryo. As the teloblasts form, they become embedded within the macromeres, which change in shape and position to partly compensate for the changes in the geometry of the D quadrant (Fig. 2D–G).

The gradual embedding of D quadrant cells in C‴ is evident by stage 5, as C‴ covers the vegetal end of the right-hand NOPQ cell, precursor to the right-hand ectodermal teloblasts (Fig. 2D). This movement shifts C‴ clockwise relative to the D quadrant progeny (compare Fig. 2C, D, G) and is accompanied by expansions of A‴ and B‴ (compare Fig. 2A and E, B and F). As a result, the overall geometry of the embryo shifts between stages 3 and 7. At stages 3–4a, cell B straddles the midline while cells A and C seem bilaterally paired across the midline; but by the end of stage 7, C‴ straddles the midline while A‴ and B‴ form a bilateral pair.

The macromere do not participate equally in enveloping the teloblasts. C‴ contacts all of the teloblasts and envelops most of them as it comes to occupy the prospective posterior region of the embryo (Fig. 2G). A‴ contacts only the two M teloblasts and the left N teloblast; the left M teloblast is almost completely embedded in A‴ while left N is covered just in its vegetal region by A‴ (Fig. 2E). B‴ contacts only the right M teloblast, which thus contacts all three macromeres (Fig. 2F). Within the β-galactosidase-stained macromeres, the teloblasts, germinal bands and germinal plate appear as clear regions (Fig. 2E–Q).

Accompanying the expansion of the macromeres, their relative positions along the animal-vegetal axis also change. A‴ and B‴ thicken and spread at the animal end of the embryo, coming to occupy most of the region under the micromere cap as they thin and retract from the vegetal end (Fig. 2J), C‴ undergoes complementary movements, receding from the animal pole and occupying more vegetal territory (Fig. 2K).

Phase II: fusion of A‴ and B‴ (stage 6a+33 h to 6a+45 h)

A‴, B‴ and C‴ generate definitive endoderm via a multinucleate syncytium (Whitman 1878; Nardelli-Haefliger and Shankland 1993). At some point in this process, the three macromeres fuse with one another, as has been evident to us and others from the fact that injected lineage tracers leak from one macromere into the others during stages 7–8. We have now found that the fusion of the macromeres occurs in a two-step process with a set time course.

The first step is the fusion of A‴ and B‴ to form a cell we designate as A/B. When we injected β-galactosidase into either the A or B quadrant macromere during stages 4–5 and then stained at progressively later times, we detected diffusion of the enzyme from one macromere into the other (as determined by the presence of blue reaction product in both cells) beginning as early as mid-stage 7 (stage 6a+33 h; Figs. 2H, I and 3). During the earliest time points at which fusion was apparent, the reaction product was more intense in the injected cell, indicating that diffusion of the injected β-galactosidase had not reached equilibrium between the recently fused cells (Fig. 2H).

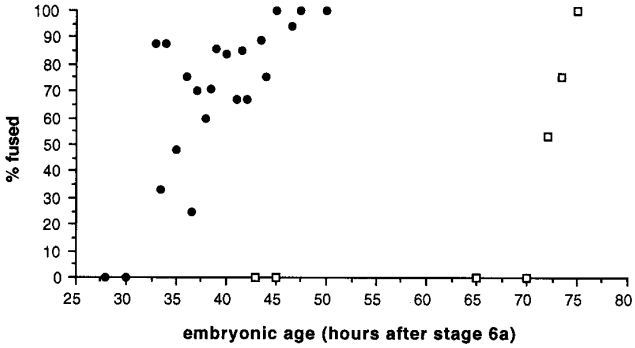

Fig. 3 Macromere fusion occurs in two discrete steps. Percent of embryos exhibiting A‴–B‴ fusion (*dots*) or A/B–C‴ fusion (*squares*) as a function of embryonic age. To assess A‴–B‴ fusion, β-galactosidase was injected into either A‴ or B‴ and embryos were scored for the diffusion of enzyme into the other cell; no diffusion into C‴ was seen. To assess A/B–C‴ fusion, β-galactosidase was injected into C‴ and embryos were scored for the diffusion of enzyme into A/B. Each time point represents the average obtained from 3–38 embryos (average sample size, 16 embryos

By stage 6a+45 h (end of stage 7), A‴ and B‴ had fused in virtually all embryos (Fig. 3), and the reaction product was of equal intensity in the two cells (Fig. 2I). In contrast, there was almost no instance of fusion with C‴ by this time. Of 256 embryos (19 experiments) in which A‴ was injected, only 1 embryo was obtained in which all 3 macromeres had fused by stage 6a+43 h. Of 70 embryos (4 experiments) in which B‴ was injected, only 2 embryos were obtained in which all 3 macromeres had fused by stage 6a+45 h. No embryos were observed in which A‴ and C‴ or B‴ and C‴ had fused selectively. Moreover, we never observed diffusion of β-galactosidase from A‴ or B‴ into any of the D quadrant derivatives during this phase.

By the time of A‴–B‴ fusion, these two macromeres form a bilateral pair with respect to the germinal bands and nascent germinal plate. The cleavage furrow separating A‴ and B‴ gradually becomes less distinct after the two cells fuse but is visible as late as stage 6a+50 h (mid stage 8). At this time, the germinal plate is approximately one-half formed, and the unfused germinal bands traversing the equatorial regions of the embryo are roughly coincided with the posterior/vegetal limit of A/B (Fig. 2L).

To observe ultrastructural changes correlated with the fusion of A‴ and B‴ we used transmission electron microscopy to examine embryos fixed at stage 6a+42 or stage 6a+55 h. In both sets of embryos, A‴–B‴ fusion had occurred by 6a+41 h, as judged by the leakage of lineage tracer from A‴ into B‴. Thus, in the two batches of experimental embryos, A‴–B‴ fusion had occurred at least 1 or 14 h prior to fixation, respectively.

In the older embryos (at least 14 h post-fusion), membranes in the zone of apposition between the original A‴ and B‴ macromeres showed gaps up to 3 μm wide (Fig. 4A) that were not observed in embryos fixed prior to fusion (data not shown). These gaps extended through mul-

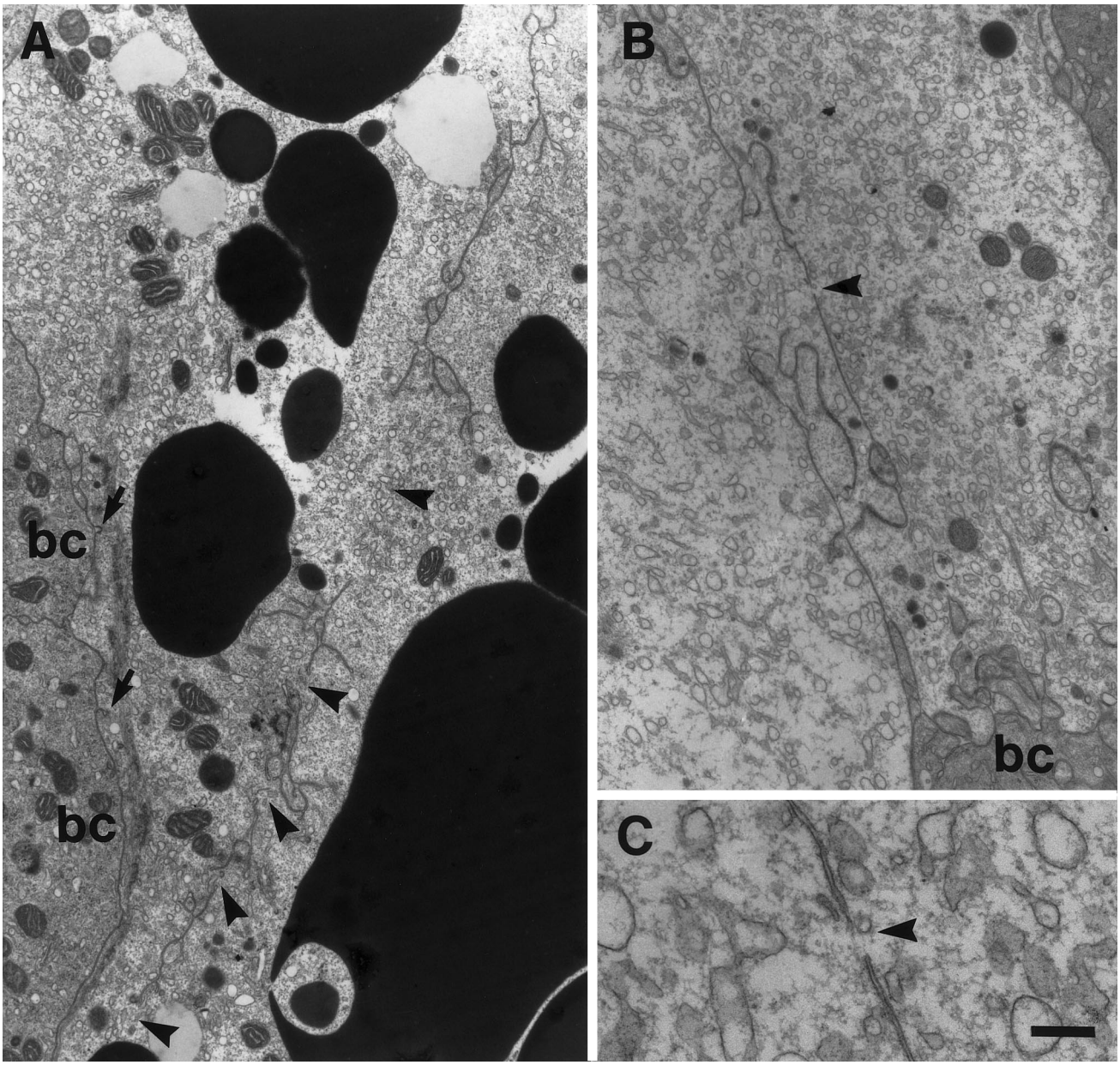

Fig. 4A–C Ultrastructural correlates of A‴–B‴ fusion. Electron micrographs of apposing A‴ and B‴ membranes during fusion. In each panel, the nominal A‴ macromere is *on the left*, B‴ is *on the right* and their apposing membranes run diagonally through the center. *Arrowheads* mark fusion pores or gaps in the membranes. **A** At stage 6a+55 h (>14 h post-fusion), there are numerous gaps in the apposing A‴ and B‴ membranes in the vicinity of the blast cells (*bc*). The A‴ and B‴ membranes interdigitate but are continuous in the upper portion of the panel and remain so all the way to the surface of the embryo (not shown). The many vesicles in the uppermost gap may be breakdown products of the plasma membranes. *Arrows* mark putative endocytic figures in the macromere membrane next to the blast cells. In the same region, a filamentous bundle courses through the macromere cytoplasm next to the blast cells. Yolk platelets are *black*. **B** In an embryo at stage 6a+42 h (>1 h post fusion), the A‴–B‴ membrane appears largely intact; a single fusion pore is visible. **C** Higher magnification of the pore in **B** (*Scale bar* **A**, **B** 1 μm, **C** 300 nm)

tiple serial sections and were bounded by islands of flattened double membrane, presumably formed by the joining of the nominal A‴ and B‴ membranes. At this stage, the gaps were only seen near where A‴ and B‴ also contact the blast cells and/or micromeres, beneath the surface at the animal end of the embryo (Fig. 4A). At the vegetal end of the embryo, and near the apical surface at the animal end, the membranes interdigitated extensively but were continuous.

In the younter embryos (at least 1 h post-fusion), no prominent gaps were observed, but we did find a single small fusion pore in one of the embryos (Fig. 4B, C). As in the older embryos, this pore was located at the animal end of the embryo, near the blast cells. No pores or gaps were observed between A‴ and C‴ or between B‴ and C‴ in either group of embryos, nor could we detect

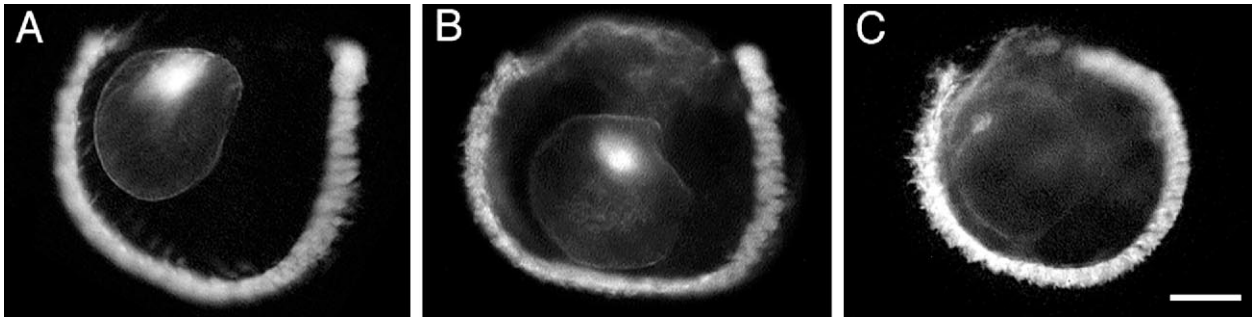

Fig. 5A–C Fusion of the left M teloblast with A/B/C to form the syncytial yolk cell. Fluorescence photomicrographs showing sagittal views of embryos, fixed at stages 6a+72, 6a+72, and 6a+86 h, respectively, in which RDA had been injected into teloblast M_L at stage 5. **A** Before M_L fuses with A/B/C, the labeled bandlet and teloblast are distinct and no fluorescence is present within A/B/C. **B** After fusion, but prior to equilibration of the lineage tracer within the syncytial yolk cell, M_L is visible, but the syncytial yolk cell is also labeled. **C** After fusion and equilibration of the lineage tracer, the outline of M_L is no longer distinct (*Scale bar* 100 μm)

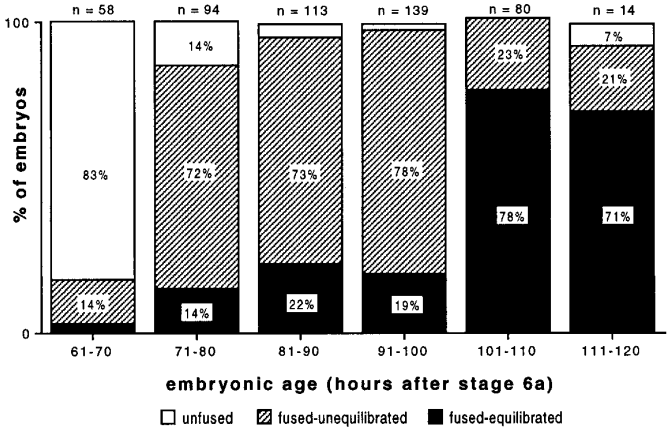

Fig. 6 Time course of teloblast M_L fusion. Percent of embryos fixed during various time intervals in which fusion of M_L either was undetectable (*clear*), had occurred without equilibration of the RDA lineage tracer (*hatching*) or had occurred with equilibration of the lineage tracer throughout the syncytial yolk cell (*solid*)

paired vesicles lined up across the apposed membranes, as seen during an early stage of myoblast fusion in *Drosophila* (Doberstein et al. 1997).

Other features of interest in the electron micrographs (Fig. 4A) included the occurrence of coated, putative endocytic figures in the macromere membrane apposing the blast cells. These correlated with what appeared to be numerous small vesicles throughout the cytoplasm of the macromere in this region. We also saw cytoskeletal fibers just beneath the membrane of the A/B cell running parallel to the blast cells.

Phase III. fusion of C‴ with A/B (stage 6a+70 h to 6a+75 h)

C‴ fuses with A/B to form cell A/B/C within a 5-h time window. This process begins approximately 25 h after the fusion of A‴ and B‴ (Fig. 3). As with A‴–B‴ fusion, injected β-galactosidase diffuses into or out of C‴ upon fusion, and embryos showing different intensities of staining between the newly fused cells are observed at the onset of fusion (Fig. 2M, N). With this second fusion event, the entire yolky region of the embryo stains blue, except that the unfused teloblasts remain distinct, giving rise to the blotchy appearance of cell A/B/C (Fig. 2Q).

Phase IV: fusion of teloblasts with A/B/C (after stage 6a+75 h)

We also examined the fusion of the teloblasts with A/B/C, designating the cell resulting from the fusion of teloblasts with A/B/C as the syncytial yolk cell. Schmidt (1939) proposed that the M teloblasts of glossiphoniid leech embryos fuse with the macromeres on the basis of light microscopic examination of sectioned embryos of somewhat indeterminate age. [Schuster (1940) reported that the outlines of the teloblasts become difficult to distinguish, but apparently did not regard this as cell fusion.] We confirmed and extended Schmidt's findings by injecting M teloblasts with lineage tracer early in stage 6, then fixing and clearing the embryos at time points beginning at the end of stage 8.

At early time points, the labeled M teloblast contrasted sharply with the surrounding, unlabeled A/B/C cells (Figs. 5A, 6). In older embryos, the syncytial yolk cell exhibited marked red fluorescence, yet the M teloblast remained as a distinctly labeled sphere (Figs. 5B, 6). We interpret this as indicating that the M teloblast had fused with A/B/C but that the lineage tracer had not yet equilibrated between the two cells. Alternatively, the label in A/B/C could represent the leakage of cytoplasmic contents from the supernumerary m blast cells (Fernandez and Stent 1982; Zackson 1982) that had either died or fused with A/B/C (Desjeux 1995).

At yet later time points, the syncytial yolk cell in most embryos was labeled uniformly (Figs. 5C, 6), suggesting that the contents of the former M teloblast and A/B/C had equilibrated by stage 6+100 h. In 20–30% of the embryos, however, the injected lineage tracer had not equilibrated between the M teloblast and A/B/C even at

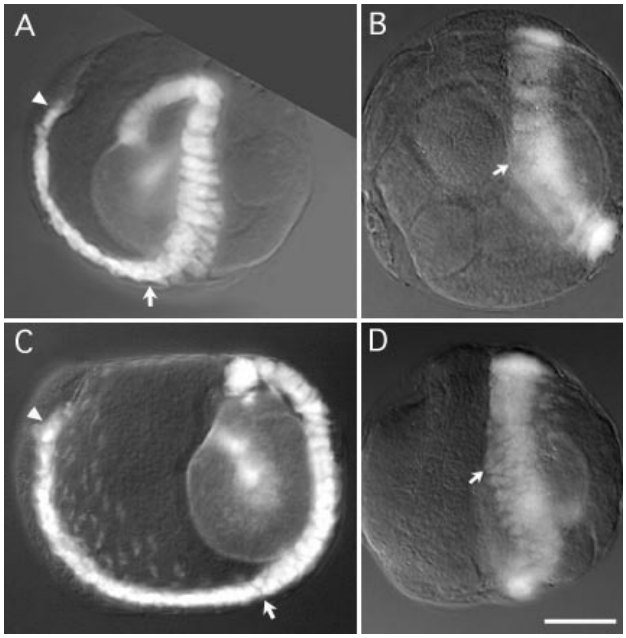

Fig. 7A–D Ricin injection into C‴ accelerates germinal band coalescence. Digitally montaged fluorescence photomicrographs of embryos, fixed at stage 6a+75 h, in which teloblast M_L had been injected with RDA at stage 6a. *Arrowheads* mark the first RDA-labeled and coalesced m clone; *arrows* mark the last coalesced clone of the forming germinal plate. **A** Sagittal view of a control embryo shows the normal extent of coalescence. **B** Ventral view of the embryo in **A** shows the characteristic kink between the germinal band (*below the arrow*) and germinal plate (*above the arrow*). **C** Sagittal view of a sibling embryo in which C‴ had been injected with ricin; the germinal plate (distance *between the arrowhead and the arrow*) is longer and M_L is displaced towards the posterior end of the embryo relative to the control (**A**). **D** Ventral view of the embryo in **C** shows that the bandlet kinks less sharply at the point of coalescence (*arrow*) than in the control (**B**), further evidence that coalescence has progressed further in the ricin-injected embryo (*Scale bar* 100 μm)

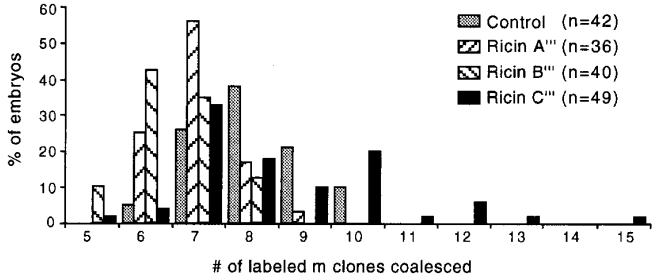

Fig. 8 Macromere-specific effects of biochemical arrest on germinal band coalescence. Germinal band coalescence was measured at stage 6a+75 h in control embryos and in embryos in which A‴, B‴ or C‴ had been biochemically arrested by the injection of ricin at stage 6a. Embryos in which ricin had been injected into C‴ (*solid*) frequently exhibited more extensive coalescence than any other group. Embryos in which ricin had been injected into A‴ or B‴ (*hatching*) typically showed less extensive coalescence than uninjected controls (*shading*)

the least stage examined (Fig. 6). This may reflect variability in the timing of the fusion process; alternatively, lineage tracer in the M teloblast may have been sequestered into cytoplasmic organelles, which would diffuse far more slowly than the free tracer.

Similar experiments, in which the left N teloblast rather than the left M teloblast was injected, reveal that these ectodermal teloblasts also fuse with the syncytial yolk cell, but do so significantly later. Fusion of the left N teloblast with the syncytial yolk cell was not observed prior to stage 6+100 h; equilibration of the lineage tracer was observed in most embryos fixed after stage 6a+123 h (data not shown). This result is consistent with the fact that while M teloblasts have produced their full complement of segmental founder cells by about stage 6a+30 h, the N teloblasts are still producing segmental founder cells until about stage 6a+65 h (Wordeman 1983; unpublished observations).

Perturbation of germinal plate formation in embryos with biochemically arrested macromeres

The A chain of ricin inhibits protein synthesis in eukaryotes (Endo and Tsurugi 1988). Macromeres injected with ricin tend to round up within a few hours of the injection, but do not lyse and do not necessarily die (Nelson and Weisblat 1992), we therefore refer to them as being "biochemically arrested". To examine the role of macromeres in germinal plate formation, we compared the rates of germinal plate formation in control embryos and in embryos in which a macromere had been injected with ricin at stage 6a. To determine these rates, we counted the number of coalesced segments in partially formed germinal plates in which the mesodermal lineage was labeled with lineage tracer to take advantage of its segmentally distinct pattern. Embryos were fixed at stage 6a+75 h, by which time control embryos without ricin injection had reached mid stage 8 (Fig. 1) and their partially formed germinal plates contained 6–10 labeled m blast cell clones (Figs. 7, 8).

The germinal plates of embryos in which either A‴ or B‴ was biochemically arrested tended to be shorter than in control embryos, with 5–9 labeled m blast cell clones (Figs. 7A, B, 8). We observed no difference between embryos in which A‴ was arrested and those in which B‴ was arrested. In contrast, the germinal plates of embryos in which C‴ was arrested were often longer than in controls, with up to 15 labeled clones (Figs. 7C, D, 8). This suggests that C‴ plays a different role than A‴ and B‴ during germinal plate formation.

We do not believe that biochemical arrest of a macromere changes the rate of primary blast cell production in teloblasts. There was no significant difference at 14.5 h after ricin injection in the number of primary blast cells born among the four classes of embryos [10.3±0.8 cells for control embryos (n=26), 10.1±1.1 cells after ricin injection into A‴ (n=24), 10.7±0.6 cells after ricin injection into B‴ (n=17) and 10.1±1.1 cells after ricin injection into C‴ (n=28)]. Embryos with ricin-injected mac-

romeres are capable of completing germinal plate formation and embryonic development, although with reduced viability; effects of ricin injection on macromere fusion depend on the time of injection and the identity of the injected cell (Isaksen 1997).

Discussion

Macromere movements during cleavage

The goal of this study was to analyze cellular behaviors of the macromeres, three large, yolk-rich, endodermal precursor cells that constitute the bulk of the early embryo in glossiphoniid leeches. We find that the macromeres undergo cell-specific spreading and shifting movements during cleavage, prior to the epibolic movements of the germinal bands and provisional integument during gastrulation.

Viewing the cell movements relative to the D quadrant derivatives as we have here, B′ and D′ straddle the prospective embryonic midline in the eight-celled embryo, while A′ and C′ are bilaterally symmetric to one another (Fig. 1, stage 4a). As cleavage proceeds, C‴ spreads clockwise to envelop most of the teloblasts as they arise from the D quadrant and occupies a somewhat more vegetal position. Macromeres A‴ and B‴ undergo similar, but less pronounced shifting and spreading movements to occupy a more animal position with respect to C‴. Thus, by stage 7, C‴ straddles the midline in prospective posterior territory, while A‴ and B‴ are bilaterally symmetric to one another in prospective anterior territory.

An alternative frame of reference for contemplating these cell movements is to keep the first cleavage plane perpendicular to the anteroposterior axis of the embryo. In this frame of reference, A and B quandrant cells are bilateral from the time of their birth and undergo spreading but no net clockwise movements, while the C and D quadrants shift clockwise and counterclockwise, respectively, as they interdigitate at the midline.

Whether one of these representations more accurately describes the active cell movements remains to be determined since the mechanisms by which the movements occur are unknown. But the process is not simply a passive accommodation by the endodermal precursors to the cleavages in the D quadrant. A‴ and C‴ both sit next to the cleaving D quadrant cells, yet C‴spreads more than A‴ or B‴, enveloping most of the teloblasts and contacting all ten, while A‴ contacts only three and B‴ contacts only one.

Macromere movements and germinal plate formation

Biochemical arrest of A‴ or B‴ by ricin injection retards germinal band coalescence slightly relative to controls, while arresting C‴ often accelerates the coalescence markedly. Because coalescence can be either accelerated or retarded by ricin injection, it is unlikely that ricin acts merely as a general poison for the embryo. Possible explanations include:

1. C‴ could inhibit the germinal band movements via a biochemical signal that is blocked by injecting that macromere with ricin. There is no direct evidence that C‴ differs biochemically from A‴ and B‴, but the differences in cell behaviors described here are consistent with this sort of explanation.
2. While the rounding up of A‴ and B‴ after ricin injection could impede the germinal band movements, the rounding up of C‴ tends to extrude the enveloped teloblasts and their progeny and might thereby accelerate germinal band formation and/or coalescence.

Macromere and teloblast fusion

In addition to the nearly universal process of sperm-egg fusion at the start of embryogenesis (Yanagimachi 1988), cell fusion occurs in the development of diverse animal taxa, with examples reported for all three germ layers. In mesoderm, for example, cells fuse during myogenesis in many animals (Knudsen 1991; but not in leech body wall muscle, Sawyer 1986), during formation of bone resorbing osteoclasts (Baron et al. 1993) and syncytiotrophoblasts in mammals (Pierce and Midgely 1963) and during sea urchin spicule formation (Hodor and Ettensohn 1996). Both ectodermal and mesodermal cell fusions have been described in nematode (Albertson and Thomson 1976; Sulston et al. 1983). As reviewed by Anderson (1973), midgut formation among different annelids (and arthrorthopods) proceeds by various strategies, some of which involve cell fusion of endodermal precursor cells.

For glossiphoniid leeches, Whitman (1878) concluded that the epithelial lining of the gut arises from multinucleate macromeres, but he seemed unaware that these cells fuse with one another, stating, “I have found that these blastomeres preserve their individuality during the entire period of invagination and neurulation …”. Fusion of yolk cells to form a syncytium which then cellularizes at the periphery to form the midgut epithelium was described clearly for glossiphoniid leeches by Bychowsky (1921), and Schmidt (1939) reported the fusion of the M teloblasts with the macromeres. Here, we used an enzyme diffusion assay to show that the macromeres fuse in a stepwise and stereotyped manner and that the mesodermal (M) and ectodermal (N) teloblasts fuse with the resultant syncytial yolk cell. Our results indicate that fusion begins much earlier than was evident to Bychowsky (1921), who apparently described late stage 9 embryos.

We have also examined fusion at the ultrastructural level, focusing on the fusion of A‴ and B‴. The first obvious breakdown of membranes between the fusing cells occurs deep beneath the surface of the embryo, near the blast cells and micromeres. Our finding is consistent with previous observations that the loss of visible yolk cell boundaries occurs with an anteroposterior progression (Bychowsky 1921), and suggests that macromere

fusion may be regulated or induced by signals emanating from the blast cells and/or micromeres.

Developmental significance of stepwise fusion

The developmental significance of the stepwise macromere fusion remains to be determined. Possibilities include:

1. The fusion of A‴ and B‴, together with the clockwise shift of these cells to occupy a bilaterally symmetric rostral position, might help to orchestrate the germinal band coalescence during early stage 8. The close correlation between the timing of A‴–B‴ fusion and the onset of germinal band coalescence is consistent with this possibility. Similarly, the timing of the fusion of A/B with C‴ correlates with the end of coalescence.
2. The stepwise fusion and the associated macromere movements may be critical steps in a process by which A‴ and B‴ come to contribute to a different part of the gut than does C‴.
3. During blast cell production, C‴ envelops the teloblasts and the portions of their bandlets than have not yet entered a germinal band. Blast cell production continues until approximately stage 6a+65 h, long after the fusion of A‴ and B‴. Thus, maintaining C‴ in a state of noncompetence for fusion during this period might ensure that the teloblasts and their blast cell progeny are not diverted prematurely to an endodermal fate by inadvertently fusing with C‴.

Near the end of blast cell production, each teloblast generates "supernumerary" blast cells that are not incorporated into germinal bands and plate. It was originally supposed that these cells die (Shankland 1984) but recent experiments suggest that they fuse with the endodermal lineage instead (Desjeux 1995; M. Shankland, in press). This would mean that D quadrant derivatives, in the form of the teloblasts and their supernumerary blast cells, also contribute to the gut epithelium, further complicating the significance of the classical germ layer designations. Thus, the processes we have described here are probably just the first of several distinct cell fusion events in which the macromeres fuse first with each other, and later with the ten teloblasts and the supernumerary blast cells to generate a syncytial yolk cell having a mixture of nuclear and cytoplasmic contributions.

Acknowledgements We thank Michael Leviten for assistance in counting m blast cell clones, Jae Hyuk Lee for determining the time course of N teloblast fusion, Françoise Huang for help with generating images, and Marc Pilon and Norris Armstrong for translating references. This work was supported by NSF grants IBN 9406141 and IBN 9723114.

References

Albertson DG, Thomson JN (1976) The pharynx of *Caenorhabditis elegans.* Philos Trans R Soc London Ser B 275:299–325

Anderson DT (1973) Embryology and phylogeny in annelids and arthropods. Pergamon Press, Oxford, pp 74–77

Baron R, Chakhraborty M, Chatterjee D, Horne W, Lomri D, Ravesboot J-H (1993) Biology of the osteoclast. In: Mundy GR, Martin TJ (eds) Handbook of experimental pharmacology, vol 107. Springer, Berlin Heidelberg New York, pp 111–148

Bissen ST, Weisblat DA (1989) The durations and compositions of cell cycles in embryos of the leech, *Helobdella triserialis.* Development 106:105–118

Bychowsky A (1921) Ueber die Entwicklung der Nephridien von *Clepsine sexoculata* Bergmann. Rev Suisse de Zool 29:41–131

Demaree RS Jr, Giberson R, Smith RL (1995) Routine microwave polymerization of resins for transmission electron microscopy. Scanning 17 (Suppl 5) 25–26

Desjeux I (1995) An investigation into the regulation of segment number in the leech. PhD thesis, Dept Physiol, University Medical School, Edinburgh

Doberstein SK, Fetter RD, Mehta AY, Goodman CS (1997) Genetic analysis of myoblast fusion: blown fuse is required for progression beyond the prefusion complex. J Cell Biol 136:1249–1261

Endo Y, Tsurugi K (1988) The RNA N-glycosidase activity of ricin A-chain: the characteristics of the enzymatic activity of ricin A-chain with ribosomes and with rRNA. J Biol Chem 263:8735–8739

Fernandez J, Stent GS (1982) Embryonic development of the hirudinid leech *Hirudo medicinalis:* structure, developmental and segmentation of the germinal plate. J Embryol Exp Morphol 72:71–96

Hirsch JG, Fedorko ME (1968) Ultrastructure of human leukocytes after simultaneous fixation with glutaraldehyde and osmium tetroxide and "postfixation" in uranyl acetate. J Cell Biol 38:615–627

Hodor PG, Ettensohn CA (1996) Cell-cell fusion in the sea urchin primary mesenchyme. Mol Biol Cell 7 (Suppl):110a

Isaksen DE (1997) The identification of a TGF-β class member and the regulation of endodermal precursor cell fusion in the leech. PhD thesis, Dept Mol Cell Biol, University of California, Berkeley

Knudsen KA (1991) Fusion of myoblasts. In: Wilschut J, Hoekstra D (eds) Membrane fusion. Marcel Dekker, New York

Nardelli-Haefliger D, Shankland M (1993) Lox 10, a member of the NK-2 homeobox gene class, is expressed in a segmental pattern in the endoderm and in the cephalic nervous system of the leech *Helobdella.* Development 118:877-892

Nelson BH, Weisblat DA (1992) Cytoplasmic and cortical determinants interact to specify ectoderm and mesoderm in the leech embryo. Development 115:103–115

Pierce GB Jr, Midgley AR Jr (1963) The origin and function of human syncytiotrophoblastic giant cells. Am J Pathol 43:153–173

Sandig M, Dohle W (1988) The cleavage pattern in the leech *Theromyzon tessulatum* (Hirudinea, Glossiphoniidae). J Morphol 196:217–252

Sawyer RT (1986) Anatomy, physiology, and behaviour. Leech biology and behaviour, vol I. Oxford Univ Press, Oxford New York, pp 229

Schmidt GA (1939) Dégénérescence phylogénétique des modes de développement des organes. Arch Zool Exp Gen 81:317–370

Schuster M (1940) Die entwicklungsgeschichtliche bedeutung der teloblasten bei *Glossiphonia complanata* L. LZ Wiss Zool Leipz 153:393–461

Shankland M (1984) Positional determination of supernumerary blast cell death in the leech embryol. Nature 307:541–543

Shankland M (in press) Specification of cell fates during leech segmentation. In: Moody S (ed) Mechanisms of cell lineage and cell fate determination. Academic Press, New York

Smith CM, Weisblat DA (1994) Micromere fate maps in leech embryos: lineage-specific differences in rates of cell proliferation. Development 120:3427–3438

Smith CM, Lans D, Weisblat DA (1996) Cellular mechanisms of epiboly in leech embryos. Development 122:1885–1894

Stent GS, Kristan WB Jr, Torrence SA, French KA, Weisblat DA (1992) Development of the leech nervous system. Int Rev Neurobiol 33:109–193

Sulston JE, Schierenberg E, White JG, Thomson JN (1983) The embryonic cell lineage of the nematode *Caenorhabditis elegans.* Dev Biol 100:64–119

Weisblat DA, Kim SY, Stent GS (1984) Embryonic origins of cells in the leech *Helobdella triserialis.* Dev Biol 104:65–85

Whitman CO (1878) The embryology of Clepsine. Q J Microsc Sci 18:215–315

Wordeman L (1983) Kinetics of primary blast cell production in the embryo of the leech *Helobdella triserialis.* Undergraduate honors thesis, Dept Mol Biol, University of California, Berkeley

Yanagimachi R (1988) Membrane fusion in fertilization, cellular transport and viral infection. In: Duzgunes N, Bonner F (eds) Current topics in membranes and transport, vol 32. Academic Press, Orlando, pp 3–43

Zackson SL (1982) Cell clones and segmentation in leech development. Cell 31:761–770